Quasielastic Light Scattering Studies of Aqueous Biliary Lipid Systems. Size, Shape, and Thermodynamics of Bile Salt Micelles†

Norman A. Mazer,* Martin C. Carey,‡ Robert F. Kwasnick, and George B. Benedek

ABSTRACT: From measurements of the autocorrelation function and the time-averaged intensity of light scattered from aqueous bile salt solutions we have deduced the mean hydrodynamic radius ($\bar{R}_h$), shape, aggregation number ($\bar{n}$), and polydispersity of bile salt micelles as a function of bile salt species, concentration, temperature, and NaCl and urea concentrations. Our data confirm that the trihydroxy bile salt taurocholate (TC) forms smaller micelles than the dihydroxy bile salts taurodeoxycholate (TDC), tauroursodeoxycholate (TUDC), and taurochenodeoxycholate (TCDC) and also show that the latter species vary in size in the following order: TDC > TCDC > TUDC. In 0.15 M NaCl the $\bar{R}_h$ and $\bar{n}$ values are weakly dependent on bile salt concentration, whereas in 0.6 M NaCl the micelles grow appreciably with increasing concentration. The extent of micellar growth increases as the temperature is lowered from 60 to 20 °C but is diminished by the addition of urea (0–6 M). The large micelles are found to be rodlike and quite polydisperse. These data are shown to be quantitatively consistent with a two-stage model of bile salt aggregation in which bile salt monomers first associate hydrophobically at the cmc to form small globular primary micelles. At higher bile salt concentrations the primary micelles then polymerize into rodlike secondary micelles. We have deduced the polymerization constant (K) for this process as a function of each physical–chemical variable. From a thermodynamic analysis of the K values, it is concluded that the driving force for secondary micelle formation is *also* an unfavorable hydrophobic interaction between the surface of the primary micelle and the aqueous solvent which is largely enthalpic in origin. It is shown that the NaCl dependence of K can be predicted from the Verwey–Overbeek theory of double layer repulsion and that the influence of urea on secondary micelle formation is consistent with experimental data for the free energy of transferring nonpolar amino acid side groups from water to urea solutions.

Over the past decade, advances in our understanding of the physical chemistry of bile and the pathogenesis of cholesterol gallstones have resulted largely from systematic phase equilibria investigations of model bile systems composed of bile salts, lecithin, and cholesterol in aqueous solvent (Small et al., 1966; Admirand & Small, 1968; Carey & Small, 1978). These studies have shown that bile salts are amphiphiles which exhibit considerable aqueous solubility and that they also have a remarkable capacity to solubilize both lecithin and cholesterol in aqueous solution. It is now appreciated that both of these properties derive from the ability of bile salt molecules to associate with each other and with molecules of lecithin and cholesterol to form simple and mixed micellar aggregates[1] (Carey & Small, 1970, 1972). These micellar properties, in turn, derive from the unusual amphiphilic structure of the bile salt molecules and the tendency of the hydrocarbon parts of the molecules to associate with other amphiphilic solutes in order to reduce hydrocarbon contact with water, the so-called hydrophobic effect (Tanford, 1972).

Although the phase equilibria studies of model bile systems have provided an important conceptual framework for visualizing the relationship of biliary lipid composition to the solubility and precipitation of cholesterol in bile, our present theoretical understanding of these phase equilibria in quantitative molecular terms has been limited by the lack of detailed information available on the size, shape, and structure of simple bile salt micelles, biliary mixed micelles, and the precipitating lecithin and cholesterol phases. Such a fundamental understanding of biliary lipid interactions is, however, vital for understanding the molecular basis of cholesterol gallstone formation and for developing new pharmacologic agents capable of dissolving gallstones. In addition, such knowledge may have substantial application in elucidating the mechanisms of hepatic bile formation and the role of bile in fat digestion and absorption.

For these reasons we undertook a systematic investigation of simple micelle formation, mixed micelle formation, and cholesterol precipitation in aqueous biliary lipid systems[2] using the technique of quasielastic light scattering spectroscopy (QLS).[3] This technique was previously employed by us to study the alkyl chain detergent sodium dodecyl sulfate ($NaDodSO_4$) (Mazer et al., 1976) and was shown to be an ideal method for characterizing micellar size, shape, and polydispersity even at the high detergent concentrations of physiologic relevance (1–10 g/dL). Moreover, by measuring these micellar properties as functions of temperature, NaCl concentration, and other additives, one can obtain information on the thermodynamics of micellar aggregation (Mazer et al., 1977) and thus gain insight into the molecular mechanisms responsible for the size and structure of the micelles.

† From the Department of Physics, Center for Materials Science and Engineering, Massachusetts Institute of Technology, Cambridge, Massachusetts 02139, and the Department of Medicine, Harvard Medical School, Gastroenterology Division, Peter Bent Brigham Hospital, Boston, Massachusetts 02115. *Received November 29, 1978.* Supported in part by NIH Research Grants No. AM 18559 and AM 00195 (M.C.C.), NSF Grant DMR 7680895-A02 to the Center for Materials Science and Engineering, M.I.T., NSF Grant 7707666-CHE (G.B.B.), and the Whitaker Health Science Fund.

* Insurance Medical Scientist Scholar sponsored by the Connecticut Mutual Life Insurance Co. Present address: Massachusetts Institute of Technology, Cambridge, MA 02139.

‡ Recipient of a Research Career Development Award (AM 00195) from the U.S. Public Health Service (National Institutes of Arthritis, Metabolism and Digestive Diseases). Present address: Peter Bent Brigham Hospital, Boston, MA 02115.

[1] The terms "simple" and "mixed" are used to denote aggregates containing one amphiphilic species (simple) vs. those containing two or more species (mixed).

[2] A preliminary report on this work has appeared (Mittal, 1977).

[3] Abbreviations used: QLS, quasielastic light scattering spectroscopy; TC, 3α,7α,12α-trihydroxy-5β-cholanoyltaurine (trivial name, taurocholate); TDC, 3α,12α-dihydroxy-5β-cholanoyltaurine (trivial name, taurodeoxycholate); TCDC, 3α,7α-dihydroxy-5β-dihydroxy-5β-cholanoyltaurine (trivial name, taurochenodeoxycholate); TUDC, 3α,7β-dihydroxy-5β-cholanoyltaurine (trivial name, tauroursodeoxycholate); cmc, critical micellar concentration; $NaDodSO_4$, sodium dodecyl sulfate.

0006-2960/79/0418-3064$01.00/0

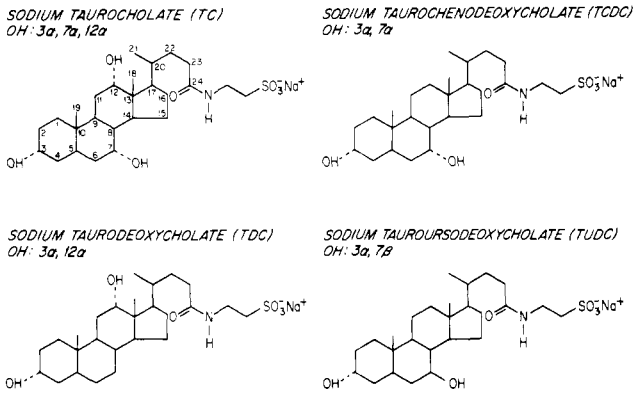

FIGURE 1: Chemical structures of the four bile salt species employed in this study. Note the differences in the number and position of the hydroxyl groups (see Matschiner, 1976).

In this paper, we report our deductions of the size, shape, aggregation number, and polydispersity of simple bile salt micelles formed by the common bile salt species of man. On the basis of these data, a quantitative model of bile salt aggregation is developed and used to derive thermodynamic information on the aggregation process. From this information the roles of electrostatic repulsion, hydrogen bonding, and hydrophobic interactions in the formation of bile salt micelles are elucidated.

Experimental Procedure

(*A*) *Materials.* The taurine conjugates of cholic (TC), deoxycholic (TDC), ursodeoxycholic (TUDC), and chenodeoxycholic (TCDC) acids were studied. These bile salts differ only in the number, position, and orientation of their hydroxyl groups (Figure 1). With the exception of TCDC, the materials were A Grade products (Calbiochem, San Diego, CA) and were purified as described (Carey & Small, 1978) to achieve at least 98% chromatographic (TLC) and potentiometric purity. The TCDC used was custom synthesized by EISAI Co., Ltd., Tokyo, Japan, and its ultrahigh purity (>99.5%) was verified on a reverse-phase, high-performance chromatograph (Bloch & Watkins, 1978). With some bile salt samples NaCl or KCl ionic contaminants (detected by flame photometry) were removed by organic solvent extraction. NaCl and urea were of ACS analytical grade quality. The NaCl was roasted in air at 600 °C for 3 h in order to oxidize and remove organic impurities. The water used was deionized, doubly distilled, and filtered to exclude dust.

(*B*) *Solutions.* Bile salt solutions were made on a w/v basis in acid-cleaned volumetric flasks with the appropriate aqueous solvent and were stored for short periods at 4°C prior to study. At this temperature the dihydroxy bile salts were observed to form gels or to precipitate from solution depending on the concentration of NaCl and bile salt species (Carey & Small, 1969; DelliColli, 1970). Such solutions were thus gently heated to dissolve either the gel or precipitate prior to making QLS measurements. No attempt was made to adjust the solution pH (which approximated neutrality) as the taurine conjugates employed are rendered insensitive to the solution pH by their low pK_a values (<2.0) (Matschiner, 1976).

(*C*) *QLS Measurements. Theory.* Quasielastic light scattering spectroscopy (QLS) is a technique which utilizes the temporal fluctuations in the intensity of the light scattered from a solution of macromolecules for measuring the translation diffusion coefficient of the macromolecules. A number of excellent reviews on the theory, instrumentation, data analysis, and applications of this technique are available in the literature (Chu, 1974; Cummins & Pike, 1974, 1977), and thus only those issues pertinent to the characterization of micellar size, polydispersity, and shape will be summarized here.

(*1*) *Micellar Size.* From a cumulant analysis (Koppel, 1972; Mazer, 1973) of the autocorrelation function of light quasielastically scattered from a micellar solution one obtains the mean diffusion coefficient of the micelles, $\bar{D}$. This quantity is a weighted average of the diffusion coefficients of all micellar species present, as defined in eq 1, where D_i is the diffusion

$$\bar{D} = \sum(G_i D_i) \tag{1}$$

coefficient of the ith micellar species and G_i is the fraction of the total light intensity scattered by that species. G_i, in turn, is given by eq 2,

$$G_i = C_i M_i P_i / \sum(C_i M_i P_i) \tag{2}$$

where C_i is the concentration (w/v), M_i is the micellar weight, and P_i is the light scattering form factor of the ith micellar species. From the $\bar{D}$ values we can deduce a measure of micellar size, the mean hydrodynamic radius, $\bar{R}_h$, by using an equation (eq 3) which is analogous to the Stokes–Einstein relation (see Mazer et al., 1976), where k is Boltzmann's

$$\bar{R}_h = kT/6\pi\eta\bar{D} \tag{3}$$

constant, T is the temperature (K), and η is the viscosity of the *solvent*. The assumptions on which eq 3 is based have been discussed in detail previously (Mazer et al., 1976, 1977). Most important of these is that the intermicellar interactions which occur in concentrated solutions have only a small influence on $\bar{D}$ due to a cancellation between thermodynamic and hydrodynamic effects and thus do not substantially affect our deductions of $\bar{R}_h$. A considerable body of experimental and theoretical information cited in our earlier work supports this assumption.

(*2*) *Micellar Polydispersity.* The cumulant analysis also provides an index of micellar polydispersity, V, defined as in eq 4, where $\overline{D^2} = \sum(G_i D_i^2)$. From this equation, it is seen that

$$V = [100 \times (\overline{D^2} - \bar{D}^2)^{1/2}/\bar{D}]\% \tag{4}$$

V gives a measure of the width of the distribution of D_i values which is normalized by the mean value, $\bar{D}$. In highly polydisperse systems, the cumulant analysis can also provide parameters which characterize the skewness and kurtosis of the distribution of D_i values (Mazer, 1973).

(*3*) *Micellar Shape.* In systems where $\bar{R}_h$ is found to depend strongly on temperature, NaCl concentration, or other variables, additional measurements of the time-average scattered light intensity, $\bar{I}$, as a function of such variables can be used to provide information on micellar shape (Mazer et al., 1976). Quantitatively analyzing the experimental dependence of $\bar{I}$ on $\bar{R}_h$ makes it possible to determine whether the micelles grow in a rodlike (prolate), disklike (oblate), or spherical fashion.

Apparatus and Methods. The apparatus and methods employed for QLS measurements are essentially the same as those described by us in detail previously (Mazer et al., 1976) with a few minor modifications. In the present study, two methods were utilized for solution clarification and cell filling. In one method, the micellar solution was filtered through a double layer of 0.1- or 0.2-μm Nuclepore membranes (A. H. Thomas Co., Philadelphia, PA) into Teflon and glass light scattering cells. In the second method, the micellar solution was pipetted into an acid-washed cylindrical scattering cell (Pyrex glass, 1-mL capacity, o.d. 5 mm) which was then stoppered and centrifuged at 12 000 rpm for 30 min (Beckman preparative ultracentrifuge, Model L) to sediment dust. When

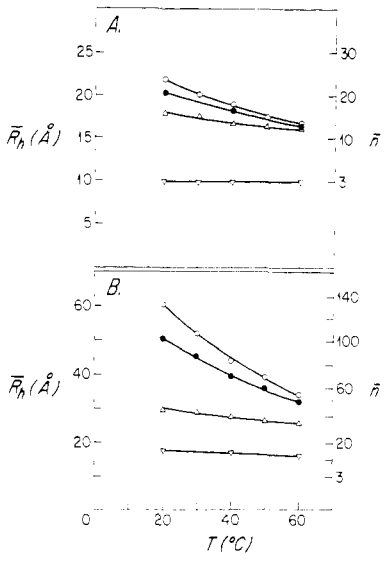

FIGURE 2: Mean hydrodynamic radii, $\bar{R}_h$, and aggregation numbers, $\bar{n}$, of bile salt micelles as functions of temperature in 10 g/dL solutions containing (A) 0.15 M NaCl and (B) 0.6 M NaCl. Bile salt species: TDC, taurodeoxycholate (○); TCDC, taurochenodeoxycholate (●); TUDC, tauroursodeoxycholate (△); and TC, taurocholate (▽).

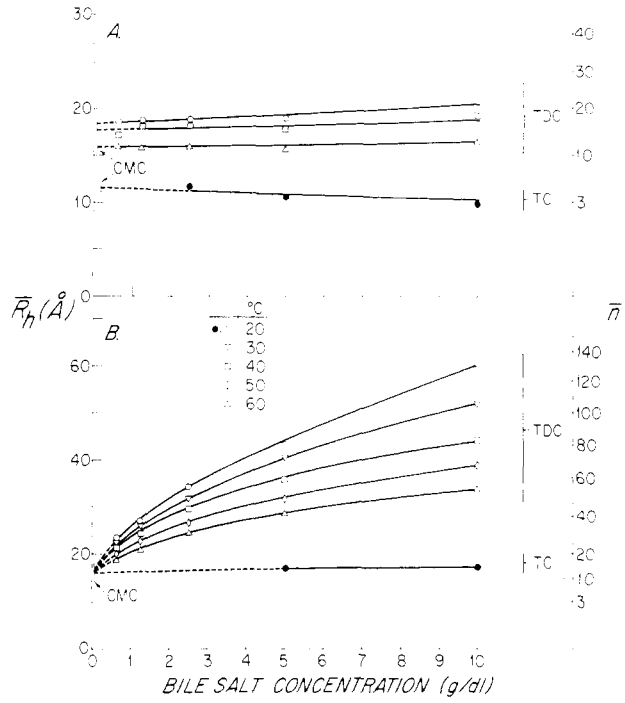

FIGURE 3: Mean hydrodynamic radii, $\bar{R}_h$, and aggregation numbers, $\bar{n}$, of TC and TDC micelles as functions of bile salt concentration in (A) 0.15 M NaCl and (B) 0.6 M NaCl, showing extrapolations to the estimated critical micellar concentration (cmc) values (Carey & Small, 1969).

compared with each other on the same sample, both methods gave identical results for $\bar{D}$ and V. The laser wavelengths employed were 5145 and 4880 Å, and the scattering angle was usually kept at 90°. When necessary, lower angles were used in order to obtain a suitable time scale for measuring the autocorrelation function. Over the accessible range of scattering angles (30–90°), no appreciable variations in $\bar{D}$ or V were found. The autocorrelator was operated in the scaling mode, utilizing 20 channels, the last four being delayed ~400 times the characteristic channel width so as to obtain a direct measurement of the base line. Cumulant analyses of the autocorrelation functions were performed on a NOVA 1200 computer. In the present experiments, nearly all of the observed autocorrelation functions could be fit by using two cumulants with a precision of better than 5 parts in 10^3 in each of the data points. With most solutions, this precision could not be improved upon in a statistically significant fashion with the addition of further cumulants. The index of refraction of the bile solutions needed for calculating the magnitude of the scattering vector k was determined by using the refractive index for water with small corrections based on the refractive increments for the bile salts, NaCl, and urea (DelliColli, 1970; Vitello, 1971).

Measurements of the time-averaged intensity, $\bar{I}$, of the scattered light were obtained by measuring the current output of the photomultiplier tube on a digital ammeter. Small corrections for background scattering were made as described elsewhere (Mazer et al., 1976).

Results

(A) Mean Hydrodynamic Radii. (1) Dependence on Bile Salt Species, Temperature, and NaCl Concentration. In Figures 2A and 2B the $\bar{R}_h$ values of TCDC, TDC, TUDC, and TC micelles are plotted as functions of temperature in 0.15 and 0.6 M NaCl, respectively. The bile salt concentration in these experiments was 10 g/dL, the typical solute concentration of gallbladder bile (Carey & Small, 1972 and 1978). At both NaCl concentrations the trihydroxy bile salt TC forms much smaller micelles ($\bar{R}_h \simeq$ 10–15 Å) than the three dihydroxy bile salts whose sizes ($\bar{R}_h \simeq$ 15–60 Å) vary markedly in the following order: TDC > TCDC > TUDC.[4] Temperature and NaCl concentrations have strong influences on the size of the dihydroxy micelles, in that increases in temperature (20 → 60 °C) produce decreases in $\bar{R}_h$, whereas increases in NaCl concentration result in substantial micellar growth. For the TC micelles, the dependence on these variables is much weaker; however, in very high NaCl concentrations (3.0 M) the size of TC micelles does grow considerably ($\bar{R}_h \simeq$ 38.5 Å at 20 °C) and decreases with increasing temperature ($\bar{R}_h \simeq$ 35.5 Å at 40 °C and 31 Å at 60 °C), similar to the dihydroxy bile salt micelles.

(2) Dependence on Bile Salt Concentration. In Figures 3A and 3B the influence of bile salt concentration on $\bar{R}_h$ is shown for TDC and TC micelles at various temperatures in 0.15 and 0.6 M NaCl concentrations, respectively. The reported cmc's (Carey & Small, 1969) for these systems are also indicated in the figures. In 0.15 M NaCl the dependence of $\bar{R}_h$ on bile salt concentration is quite weak for both bile salt species (Figure 3A). Linear extrapolations of the $\bar{R}_h$ values to the cmc result in $\bar{R}_h$ values which are within 15% of the values measured at 10 g/dL. For TDC the minimum $\bar{R}_h$ values are between 16 and 18.5 Å depending on temperature, whereas for the TC micelles the extrapolated value is about 11 Å. In 0.6 M NaCl (Figure 3B), the $\bar{R}_h$ of TC micelles continues to show little dependence on bile salt concentration. However, at this high NaCl concentration, bile salt concentration does influence the size of TDC micelles, whose $\bar{R}_h$ values are seen to increase from two- to fourfold with TDC concentration depending on the temperature. Linear extrapolations of $\bar{R}_h$ to the cmc in 0.6 M NaCl were made by plotting the $\bar{R}_h$ values for TDC as a function of the square root of the bile salt concentration, $[BS]^{1/2}$. The extrapolated values obtained, 15–17 Å, are found to be nearly the same as the $\bar{R}_h$ values

[4] It should be noted that the micellar sizes and thermodynamic data reported for TCDC in this paper differ substantially from the values given by Mazer (1978). We believe the latter data to be in error due to previously unrecognized sample contamination with excess NaCl.

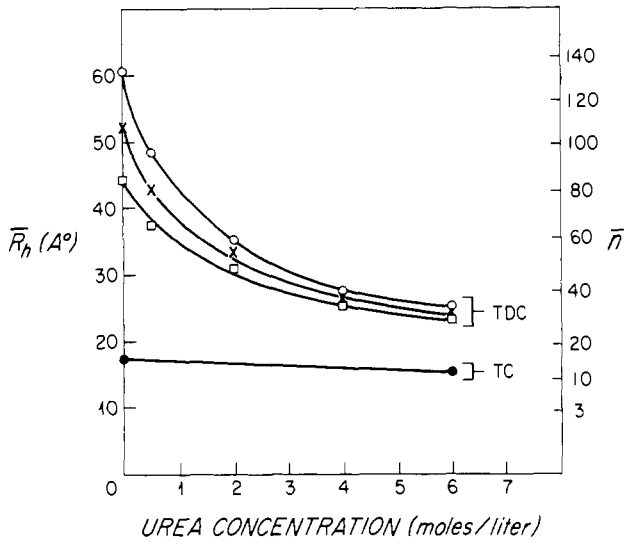

FIGURE 4: Mean hydrodynamic radii, $\bar{R}_h$, and aggregation numbers, $\bar{n}$, of TDC and TC micelles (10 g/dL, 0.6 M NaCl) as a function of urea concentration: (○, ●) 20, (x) 30, and (□) 40 °C.

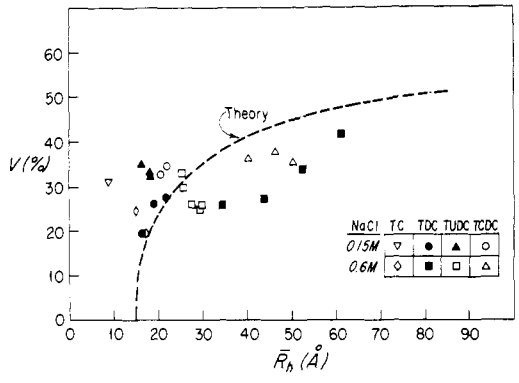

FIGURE 5: Index of micellar polydispersity, V, plotted as a function of $\bar{R}_h$ for all four bile salt species. Dashed curve represents theoretical plot of V vs. $\bar{R}_h$ based on the primary–secondary micelle theory.

extrapolated to the cmc for TDC micelles in 0.15 M NaCl.

(*3*) *Dependence on Urea Concentration.* To study the influence of a protein denaturing agent (Tanford, 1969) on bile salt micelle formation, we measured the dependence of $\bar{R}_h$ on urea concentration for 10 g/dL TDC and TC solutions in 0.6 M NaCl, and the results are shown in Figure 4. The addition of urea in concentrations up to 6 M causes a progressive reduction in $\bar{R}_h$ for the large TDC micelles measured at 20, 30, and 40 °C. For the small TC micelles urea produces only a slight decrease in size.

(*B*) *Polydispersity.* In Figure 5 the V values measured on all four bile salt species at 10 g/dL in 0.15 and 0.6 M NaCl (20–60 °C) are plotted vs. the corresponding $\bar{R}_h$ values. Although there is some scatter in V values corresponding to the same $\bar{R}_h$, one observes the general tendency for V to increase from ~20 to ~45% as the mean micellar size increases from 15 to 60 Å. This behavior is in qualitative agreement with the theoretical dependence of V on $\bar{R}_h$ predicted by the model of bile salt aggregation presented later.

(*C*) *Deductions of Micellar Shape and Aggregation Numbers.* In order to obtain information on micellar shape, measurements of the time-averaged scattered intensity $\bar{I}$ were obtained as a function of temperature (20–60 °C) for solutions containing 2.5, 5, and 10 g/dL TDC in 0.6 M NaCl. These data are plotted in Figure 6A as intensity ratios $\bar{I}(T)/\bar{I}(60\ °C)$ (T = 20, 30, 40, 50 °C) vs. the corresponding $\bar{R}_h$ value. In this way we obtain three experimental curves which can each

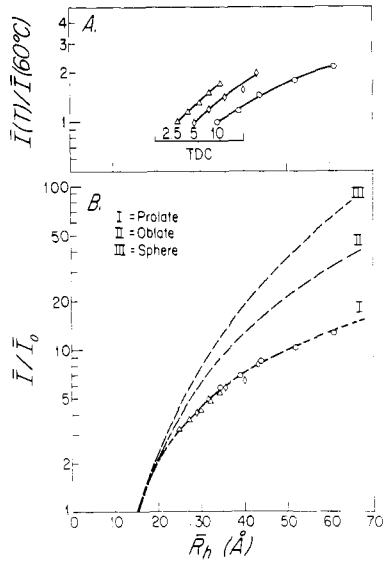

FIGURE 6: (A) Experimental intensity ratios $\bar{I}(T)/\bar{I}(60\ °C)$ (T = 20, 30, 40, 50, and 60 °C) plotted vs. the corresponding $\bar{R}_h$ values for large TDC micelles in 0.6 M NaCl. Inscribed numerals refer to the bile salt concentrations (g/dL). (B) Theoretical plots of intensity ratio vs. $\bar{R}_h$ assuming different models of micellar shape: (I) prolate ellipsoid (semiminor axis, b = 15 Å); (II) oblate ellipsoid (b = 15 Å); and (III) sphere. Experimental data of Figure 6A are seen to fit well to the prolate shape.

be used for testing different models of micellar shape. For an analysis of these data, theoretical curves of the dependence of scattered intensity on $\bar{R}_h$ were calculated [see Mazer et al. (1976) for details] by assuming the micellar shape to be (1) a prolate ellipsoid with a semiminor axis of 15 Å, (2) an oblate ellipsoid with a semiminor axis of 15 Å, and (3) a sphere. The theoretical intensity curves[5] are plotted in Figure 6B as intensity ratios $\bar{I}/\bar{I}_o$, where $\bar{I}_o$ represents the intensity associated with a solution of spherical micelles of radius 15 Å. This radius corresponds to the asymptotic minimum $\bar{R}_h$ value obtained experimentally for bile salt micelles in 0.6 M NaCl by extrapolation to the cmc and was chosen for this reason. To deduce micellar shape, an attempt was made to fit each of the experimental curves to each of the three theoretical curves. This was done graphically by simply translating the experimental curves (Figure 6A) along the vertical axis of the theoretical curves (Figure 6B) to achieve the best "fit". In this manner, it was found that each of the experimental curves superimposed best on the theoretical curve for the prolate shape as shown in Figure 6B. This finding provides compelling evidence that the large TDC bile salt micelles with $\bar{R}_h$ values between 15 and 60 Å are elongated structures with a semiminor axis of ~15 Å. With regard to the shape of the small TC micelles ($\bar{R}_h$ < 15 Å), our analysis cannot provide any information; however, intrinsic viscosity measurements in this system (Fontell, 1971; Vitello, 1971) in 0.15 M NaCl suggest that the micelles are globular and highly hydrated.

The deduction of the prolate shape for the large bile salt micelles and the assumption of a globular shape for the small micelles make it possible to estimate a mean aggregation number $\bar{n}$ (average number of bile salt molecules per micelle) corresponding to each $\bar{R}_h$. If the possible influence of bile salt species, temperature, and NaCl concentration on the hydration and density of the bile salt micelle is neglected, the functional dependence between $\bar{n}$ and $\bar{R}_h$ will be given by eq 5,

[5] The theoretical curves incorporate small corrections based on the scattering form factors for the various micellar shapes. However, this effect is appreciable only in the case of the prolate shape.

$$\bar{n} = n_o(\bar{R}_h/15)^3 \text{ for } \bar{R}_h < 15 \text{ Å}$$
$$\bar{n} = n_o[a(\bar{R}_h)/15] \text{ for } \bar{R}_h \geq 15 \text{ Å} \quad (5)$$

where n_o is the aggregation number corresponding to a spherical micelle with a hydrodynamic radius of 15 Å and $a(\bar{R}_h)$ is the semimajor axis (in Å) of the prolate ellipsoid with a hydrodynamic radius $\bar{R}_h$ and a semiminor axis of 15 Å. We have taken the value of n_o to be 10 based on calculations of the aggregation number for a spherical bile salt micelle of radius 15 Å and the range of experimental aggregation numbers (7–14) obtained for bile salt micelles of this size (Small, 1968; Vitello, 1971). Using eq 5 with $n_o = 10$, we have constructed on the right-hand sides of Figures 2–4 a nonlinear scale for estimating the mean aggregation numbers, $\bar{n}$, for the bile salt micelles. We find that the $\bar{n}$ values obtained in this study range from 3 for the small TC micelles in 0.15 M NaCl (Figure 2A) to 140 for the large TDC micelles in 0.6 M NaCl, 20 °C (Figure 2B). It must be recognized, however, that an uncertainty of at least ±30% accompanies these deductions due to uncertainties in n_o and the assumptions implicit in eq 5. With regard to the manner in which polydispersity influences $\bar{n}$, it can be shown that the $\bar{n}$ values derived from eq 5 will approximately correspond to a weight-average aggregation number (Mazer, 1978).

Discussion

(A) Comparison with Previous Deductions of Micellar Size, Shape, Aggregation Number, and Polydispersity. The present QLS study clearly demonstrates that the size, shape, aggregation number, and polydispersity of bile salt micelles depend markedly on such variables as bile salt species, temperature, NaCl concentration, bile salt concentration, and urea concentration. In this regard our data confirm many of the trends observed by Small (1967) using equilibrium ultracentrifugation and conventional light scattering methods and furthermore extend this earlier work to higher bile salt concentrations and to new bile salt species such as TUDC, presently being tested as a gallstone dissolving agent (Makino et al., 1975; Carey, 1975). In contrast with previous work, however, our data suggest some new and, in some cases, different findings. First, we note that while previous studies (Ekwall et al., 1959; Small, 1968; Carey & Small, 1972) have contrasted the micellar properties of trihydroxy bile salts with various dihydroxy bile salts, we find that the latter species also differ widely in their micellar size and dependence on temperature and NaCl concentration. Secondly, we have found that unlike the shape of small bile salt micelles ($\bar{R}_h < 15$ Å), which is probably globular (Vitello, 1971), the shape of large micelles ($\bar{R}_h \simeq 15$–60 Å) is most consistent with an elongated or rodlike structure. Thirdly, in contrast with the results of conventional light scattering (Kratohvil & Dellicolli, 1968), our study suggests that, under certain experimental conditions, the bile salt conentration can exert a profound influence on the micellar size. Finally, we have experimentally determined for the first time the polydispersity of bile salt micelles and have found that the width of the micellar size distribution can be quite large (±50% of the mean value).

With regard to the numerical values obtained for the hydrodynamic radii and aggregation numbers of bile salt micelles, our QLS measurements of TC ($\bar{R}_h = 10$ Å; $\bar{n} = 3 \pm 1$) and TDC ($\bar{R}_h = 22$ Å; $\bar{n} = 20 \pm 6$) micelles in 0.15 M NaCl (10 g/dL, 20 °C) are in good agreement with the results obtained in a number of previous studies using conventional techniques: $R_h = 9.6$–11.5 (TC) and 20–24 Å (TDC); $n = 4$–8 (TC) and 22–24 (TDC) (Woodford, 1969; Vitello, 1971; Sehlin et al., 1965; Dietschy, 1968; Small, 1968; Laurent & Persson, 1965; Borgström, 1965; Kratohvil & DelliColli, 1968; Olson & Herron, 1964). Recently, however, Holzbach et al. (1977) have obtained hydrodynamic radii for TC (21 Å) and TDC (28 Å) micelles by using QLS that are in poor agreement with both the present and previous data. In addition, they have found an anomalous concentration dependence for the diffusion coefficient of TDC micelles in 0.15 M NaCl, which is also inconsistent with the present work. The basis for these discrepancies is at present unresolved.

In comparing data obtained at high NaCl concentrations (≥0.5 M NaCl) with earlier work, one must pay particular attention to the bile salt concentration employed in the previous studies as this can affect micellar size. In this regard the extensive tabulation of aggregation numbers obtained by Small was for the most part measured at concentrations between 1 and 2 g/dL and did not represent extrapolations to the cmc (D. M. Small, personal communication). Taking this into account, we see that our $\bar{n}$ value of 45 deduced at 1.5 g/dL for TDC in 0.6 M NaCl (20 °C) (Figure 3B) is in good agreement with Small's value of 47 obtained in 0.5 M NaCl. On the other hand, the aggregation number of 50 reported by Kratohvil & DelliColli (1968) for TDC micelles in 0.5 M NaCl represents an extrapolation of turbidity measurements to the cmc and is in poor agreement with our value of 17 derived by extrapolation to the cmc in 0.6 M NaCl (Figure 3B). Moreover, these conventional light scattering measurements fail to demonstrate any dependence of aggregation number on bile salt concentration. We believe that this apparent inconsistency between the QLS results and the conventional light scattering measurements is attributable to the effect of intermicellar interactions on the turbidity measurements, which has been shown by Mukerjee (1972) to obscure the influence of detergent concentration on micellar aggregation and to introduce substantial errors in extrapolating turbidity data to the cmc. A quantitative estimate of this effect for TDC micelles in 0.6 M NaCl (Mazer, 1978) shows that the influence of excluded volume interactions between rodshaped micelles can provide a possible explanation for the results obtained by Kratohvil & DelliColli (1968).

Although there appears to be no other direct experimental data in the literature concerning the shape of large bile salt micelles ($\bar{R}_h > 15$ Å), we believe that our deduction of the rodlike shape is indirectly supported by the observation that TDC solutions in 0.6 M NaCl form gels at 4 °C. A similar gelation of bile salts has been observed at room temperature when sodium deoxycholate solutions at low ionic strengths are acidified below pH 7 (Sabotka & Czeczowezka, 1958). X-ray diffraction (Rich & Blow, 1958) and electron microscopy (McCrea & Angerer, 1960; Ramonathan et al., 1961) on these acidified bile salt gels reveal the presence of long helical fibers having a cross-sectional radius of about 20 Å. The apparent similarity between the dimensions of the helical fibers and the large TDC micelles observed here suggests that the gelation phenomena in acidified deoxycholate solutions and in TDC solutions containing 0.6 M NaCl at 4 °C have much in common and are probably the result of extensive growth of the rodlike micelles with some degree of intertwining or cross-linking between them.

(B) Thermodynamic Analysis of Bile Salt Aggregation. In this section we develop a mathematical model of bile salt aggregation based in part on the primary–secondary micelle hypothesis (Small, 1968) and also incorporating the experimental findings of the present work. Using this model, we shall derive thermodynamic information on bile salt aggregation

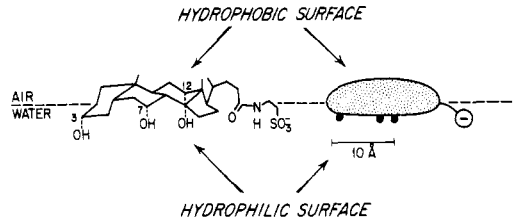

FIGURE 7: Amphiphilic structure of the trihydroxy bile salt taurocholate at an air–water interface to indicate the hydrophilic and hydrophobic surfaces of the molecule. A perspective drawing of the structure is shown on the left and a schematic model on the right.

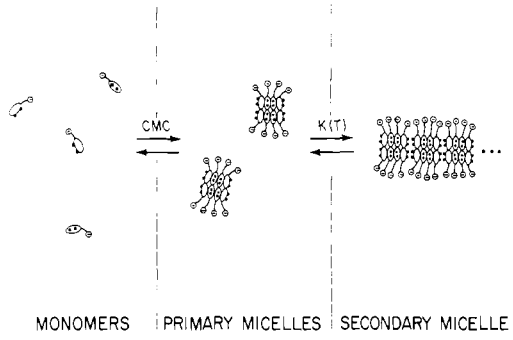

FIGURE 8: Schematic diagram of bile salt aggregation based on the primary–secondary micelle hypothesis (see text for details).

from a quantitative analysis of the dependence of $\bar{R}_h$ on bile salt concentration, bile salt species, temperature, and NaCl and urea concentrations. This information, in turn, will be used to assess the roles of electrostatic repulsion, hydrogen bonding, and hydrophobic interactions in the formation of bile salt micelles.

Primary–Secondary Micelle Hypothesis. The primary–secondary micelle hypothesis provides a conceptual model for the structure of bile salt micelles, which is predicated largely on the novel amphiphilic structure of the bile salt monomer. As shown in Figure 7, the bile salt monomer lies flat at an air–water interface with the convex surface of the steroid nucleus in contact with the lipophilic environment and the polyhydroxylated concave surface in contact with the aqueous medium. In this way the bile salt monomer displays a planar polarity with one surface being hydrophobic and the opposite surface rendered hydrophilic by the presence of the hydroxyl and ionized polar groups. According to Small, the initial stage of bile salt aggregation involves the formation of globular *primary* micelles in which the constituent molecules have their hydrophobic surfaces facing the interior of the micelle and their hydrophilic surfaces in contact with the solvent (Figure 8). Using Stuart–Briegleb molecular models, Small (1968) found that a maximum of ten bile salts could be hydrophobically associated in this manner without creating a cavity in the structure. To account for larger aggregates, Small postulated the formation of *secondary* bile salt micelles, formed by polymerization of the primary micelles, presumably via intermicellar hydrogen bonding between hydroxyl groups. Our deduction of micellar shape suggests that these large secondary micelles are rodlike, implying that the polymerization occurs in a linear fashion (shown schematically in Figure 8). Although the precise role of hydrogen bonding has not been conclusively established in aqueous bile salt solutions (Oakenfull & Fisher, 1977), it is evident that the formation of the large secondary micelles must involve some kind of interaction between the hydrophilic surfaces of the bile salt molecules (Ekwall et al., 1959). It is only in this way that one can account for the variation in micellar size among the four bile salt species studied, which differ only in the number and positioning of hydroxyl groups on their hydrophilic surface (Figure 1).

Our quantitative model of primary and secondary micelle formation begins with the simplifying assumption that the bile salt monomers, D_1, are in equilibrium with only one species of the primary micelle, D_{n_o} (eq 6),

$$n_o D_1 \overset{K_{n_o}}{\rightleftharpoons} D_{n_o} \tag{6}$$

where n_o is the aggregation number of the primary micelles and K_{n_o} is the association constant for primary micelle formation, given by eq 7, where μ°_1 and $\mu^\circ_{n_o}$ are the standard

$$K_{n_o} = \exp[-(\mu^\circ_{n_o} - n_o\mu^\circ_1)/RT] \tag{7}$$

chemical potentials of the monomer and primary micelle, respectively. Although n_o may depend slightly on bile salt species, NaCl concentration, and temperature, we will employ a single n_o equal to 10, a value consistent with our experimental observation that the $\bar{n}$ value of TDC micelles when extrapolated to the cmc approaches a minimum of 10 (i.e., $\bar{R}_h \approx 15$ Å). If the law of mass action is applied to eq 6, the equilibrium concentrations of monomers, X_1, and primary micelles, X_{n_o}, expressed in mole ratio units (i.e., moles of solute/mole of solvent), will be related by eq 8. It is this monomer–primary

$$X_{n_o} = K_{n_o}(X_1)^{n_o} \tag{8}$$

micelle equilibrium that we presume gives rise to the cmc phenomena observed in bile salt solutions in the 0.05–0.2 g/dL concentration range (Carey & Small, 1969). In fact, it can be shown that the cmc (in mole fraction units) will be approximately equal to $K_{n_o}^{-1/(n_o-1)}$ (Debye, 1949). Although recent studies (Mukerjee & Cardinal, 1976; Djavanbakht et al., 1977) suggest that the early stages of bile salt aggration may be more complex than the formulation given above, this simple treatment will be sufficient for our subsequent analysis of secondary micelle formation.

The formation of secondary micelles is modeled in eq 9 as a succession of stepwise polymerization reactions, where S_{in_o}

$$\begin{aligned} D_{n_o} + D_{n_o} &\overset{K}{\rightleftharpoons} S_{2n_o} \\ S_{2n_o} + D_{n_o} &\overset{K}{\rightleftharpoons} S_{3n_o} \\ &\vdots \\ S_{(i-1)n_o} + D_{n_o} &\overset{K}{\rightleftharpoons} S_{in_o} \\ &\vdots \end{aligned} \tag{9}$$

represents a secondary micelle composed of i primary micelles. The polymerization constant K is assumed to be the same for each reaction and therefore can be expressed in terms of the dimerization of two primary micelles (first line of eq 9) as shown in eq 10, where $\mu^\circ_{2n_o}$ is the standard chemical potential

$$K = \exp[-(\mu^\circ_{2n_o} - 2\mu^\circ_{n_o})/RT] \tag{10}$$

of the dimer state. This assumption is consistent with the behavior of other macromolecular systems in which linear polymerization occurs (Cohen & Benedek, 1976). Applying the law of mass action to the polymerization reactions, we obtain expressions for the equilibrium concentrations of the secondary micelles, X_{in_o} (eq 11), which can be solved iteratively

$$\begin{aligned} X_{2n_o} &= K(X_{n_o})^2 \\ X_{in_o} &= KX_{(i-1)n_o}X_{n_o} \quad (i = 3, 4, \ldots) \end{aligned} \tag{11}$$

to yield eq 12. Material conservation provides an additional

$$X_{in_o} = K^{-1}(KX_{n_o})^i \quad (i = 2, 3, \ldots) \tag{12}$$

constraint, relating the total bile salt concentration C_o (expressed as a mole fraction of bile salt monomers) to the equilibrium concentrations of monomers, primary micelles, and secondary micelles (eq 13). Substituting eq 12 into eq 13 and

$$C_o = X_1 + n_o X_{n_o} + \sum_{i=2}(in_o)X_{in_o} \tag{13}$$

performing the infinite sum, one obtains eq 14. Together eq

$$C_o = X_1 + n_o X_{n_o}/(1 - KX_{n_o})^2 \tag{14}$$

8, 12, and 14 determine the concentrations X_1, X_{n_o}, and X_{in_o} ($i = 2, 3, \ldots$) in terms of C_o and the equilibrium constants K_{n_o} and K. However, in the limit where C_o is much greater than the cmc, one can neglect the monomer concentration in eq 14 and thereby obtain an expression for X_{n_o} in terms of K and C_o (eq 15).

$$X_{n_o} = K^{-1}[1 - [(4KC_o/n_o + 1)^{1/2} - 1]/(2KC_o/n_o)] \tag{15}$$

If this result is substituted into eq 12, it can be seen that the relative concentrations of primary and secondary micelles will depend on the parameters K and C_o solely in terms of the product KC_o/n_o. The factor K^{-1} in eq 12 and 15 simply scales all micellar concentrations by the same amount. Having determined the mole ratios of primary and secondary micelles in terms of KC_o/n_o, one can then use eq 1–4 to calculate the theoretical $\bar{R}_h$ and V values that would be obtained for such a distribution of linear polymers in a QLS experiment. In Figure 9, the theoretical dependencies of $\bar{R}_h$ and V on KC_o/n_o obtained by computer calculations (see Appendix A) are plotted. It is seen that for $KC_o/n_o < 1$, $\bar{R}_h$ is nearly independent of the product KC_o/n_o and remains close to the minimum value of 15 Å. In this regime, the bile salt concentration, C_o, has only a weak effect on $\bar{R}_h$ and the micellar polydispersity is small ($V < 30\%$). Conversely, for $KC_o/n_o > 1$ the $\bar{R}_h$ value increases strongly with increases in KC_o/n_o, and the V value approaches 60%. In this regime, the mean value and breadth of the micellar size distribution both become large as either C_o or the polymerization constant K increases.

Analysis of the Concentration Dependence of $\bar{R}_h$. As a quantitative test of our model of primary–secondary micelle equilibrium we attempted to fit the experimental concentration dependence of $\bar{R}_h$ for TDC micelles in 0.6 M NaCl at 20, 30, 40, 50, and 60 °C with theoretical curves derived from Figure 9. The theoretical curves were obtained by empirically finding the value of K at each temperature which allowed the best agreement between the experimental and functional dependence of $\bar{R}_h$ on KC_o/n_o given in Figure 9. The very close agreement obtained at each temperature is shown in Figure 10, along with the deduced values for K. This successful comparison between theory and experiment provides compelling support for our model of micellar growth and specifically shows that the strong dependence of $\bar{R}_h$ on TDC concentration in 0.6 M NaCl is consistent with the influence of bile salt concentration on the micellar size distribution in the limit of $KC_o/n_o > 1$. Accepting the validity of our model, one can then attribute the influences of temperature, bile salt species, NaCl concentration, and urea concentration on the $\bar{R}_h$ values measured at a single bile salt concentration (i.e., 10 g/dL) to the changes these variables produce on the polymerization constant K.

Deductions of the Polymerization Constant K. Using the data of Figures 2, 3, and 5 we have deduced values for K by first determining the product KC_o/n_o corresponding to each $\bar{R}_h$ value (Figure 9) and then dividing through by the appropriate value of C_o/n_o (expressed in mole ratio units). In

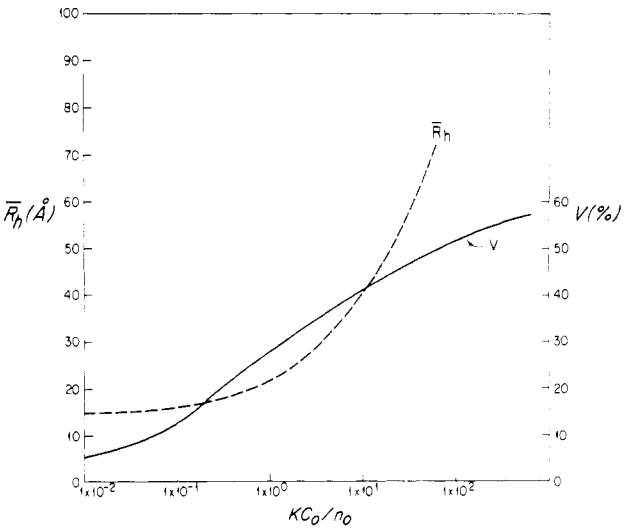

FIGURE 9: Theoretical dependence of $\bar{R}_h$ (dashed curve) and V (solid curve) on KC_o/n_o (see text for derivation).

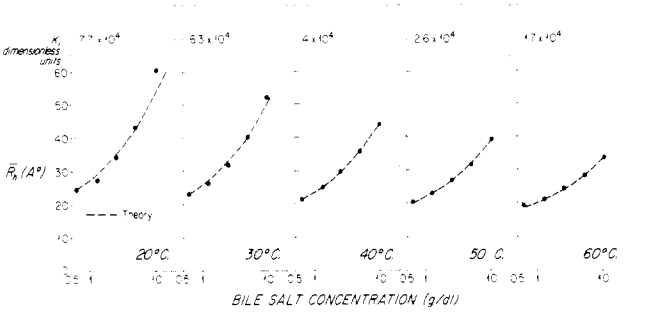

FIGURE 10: Fit of the theoretical concentration dependence of $\bar{R}_h$ to the experimental data for TDC micelles in 0.6 M NaCl at 20, 30, 40, 50, and 60 °C. The binding constant K, appropriate to each temperature, is also shown. These are computed in dimensionless units by expressing the concentration C_o as a mole ratio.

Figures 11A and 11B our deductions of ln K for the dihydroxy bile salts TCDC, TDC, and TUDC are plotted as functions of the inverse Kelvin temperature, T^{-1}, in 0.15 and 0.6 M NaCl, respectively. In Figure 11C a similar plot is made for the polymerization constant of TC micelles in 0.6 and 3.0 M NaCl, while in Figure 11D the effect of added urea concentration on the ln K values for TDC micelles in 0.6 M NaCl is shown. In all cases the plots are well described by straight lines over the temperature range 20–60 °C, with slopes that depend markedly on bile salt species and urea concentration but only weakly on NaCl concentration.

Thermodynamic Analysis of the K Values. From eq 10 it is seen that the K values given in Figure 11 can be used to deduce the change in standard chemical potential, $\Delta\mu°$, associated with the binding of two primary micelles (eq 16). The

$$\Delta\mu° \equiv \mu°_{2n_o} - 2\mu°_{n_o} = -RT \ln K \tag{16}$$

enthalpic, $\Delta H°$, and entropic, $\Delta S°$, contributions to $\Delta\mu°$ can also be obtained from the temperature dependence of K by using the thermodynamic relations shown in eq 17a and 17b (Moore, 1962), where $H°_{n_o}$, $S°_{n_o}$ and $H°_{2n_o}$, $S°_{2n_o}$ represent

$$\Delta H° \equiv H°_{2n_o} - 2H°_{n_o} = -Rd \ln K/d(1/T) \tag{17a}$$

$$\Delta S° \equiv S°_{2n_o} - 2S°_{n_o} = (\Delta H° - \Delta\mu°)/T \tag{17b}$$

the standard enthalpy and entropy of the primary and secondary micelle (dimer), respectively. As the dependence of ln K on T^{-1} was found to be approximately linear, it follows from eq 17a and 17b that the values of $\Delta H°$ and $\Delta S°$ will be

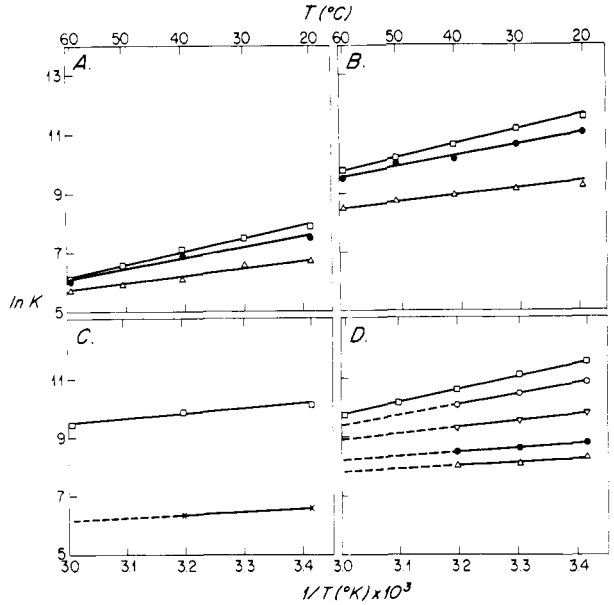

FIGURE 11: Dependence of ln K on inverse temperature [$1/T$ (K)] for various bile salt species and solvent conditions. (A) (□) TDC, (●) TCDC, and (△) TUDC in 0.15 M NaCl. (B) Same species as in (A) in 0.6 M NaCl. (C) TC micelles: (□) 3.0 M NaCl; (x) 0.6 M NaCl. (D) TDC micelles in 0.6 M NaCl at various urea concentrations (M): (□) 0; (○) 0.5; (▽) 2.0; (●) 4.0; (△) 6.0. It should be noted that the K values shown for TDC micelles in 0.6 M NaCl at 20 and 30 °C (Figure 11B) differ slightly from the values given in Figure 10 due to the fact that the former values are obtained from $\bar{R}_h$ at a single bile salt concentration, 10 g/dL, whereas the latter values are derived from fitting the entire concentration dependence of $\bar{R}_h$.

Table I: Thermodynamic Parameters of Secondary Micelle Formation

BS[a] species	solvent	$\Delta\mu°$(20 °C) (kcal/mol)	$\Delta H°$ (kcal/mol)	$\Delta S°$ ((cal/mol)/deg)
TC	0.6 M NaCl	−3.8 ± 0.3	−2 ± 0.2	5.3 ± 0.6
	3.0 M NaCl	−5.9 ± 0.6	−3.3 ± 0.4	8.9 ± 1.4
TUDC	0.15 M NaCl	−3.9 ± 0.4	−4.9 ± 0.3	−3.3 ± 0.3
	0.6 M NaCl	−5.5 ± 0.3	−4.0 ± 0.2	5.0 ± 0.5
TCDC	0.15 M NaCl	−4.4 ± 0.4	−7.2 ± 0.3	−7.2 ± 1
	0.6 M NaCl	−6.4 ± 0.3	−6.8 ± 0.2	−1.3 ± 0.3
TDC	0.15 M NaCl	−4.6 ± 0.7	−8.8 ± 0.5	−14.5 ± 1.5
	0.6 M NaCl	−6.7 ± 0.3	−9.0 ± 0.2	−7.7 ± 0.7
	+ 0.5 M urea	−6.4 ± 0.2	−7.3 ± 0.1	−3.2 ± 0.4
	+ 2 M urea	−5.7 ± 0.2	−4.1 ± 0.1	5.5 ± 0.2
	+ 4 M urea	−5.1 ± 0.2	−2.8 ± 0.1	7.9 ± 0.4
	+ 6 M urea	−4.9 ± 0.7	−2.6 ± 0.5	7.7 ± 1.6

[a] BS, bile salt.

independent of temperature. We therefore list in Table I the values (±uncertainties) of $\Delta\mu°$ (20 °C), $\Delta H°$, and $\Delta S°$ for the different bile salt species and solvent conditions investigated. From these data it is seen that the standard chemical potential of the dimer state, $\mu°_{2n_0}$, is from 3.8 to 6.7 kcal/mol lower than the chemical potential of the dissociated monomer state, $2\mu°_{n_0}$, and that the stability of the dimer is in large part due to a favorable enthalpy change (i.e., heat is given off when the primary micelles associate). In 0.6 M NaCl, the $\Delta\mu°$ values for TCDC and TUDC lie approximately within 1 kcal/mol of the value for TDC, indicating that the positioning of the two hydroxyl groups on the steroid nucleus produces relatively small changes in the value of $\Delta\mu°$. Nevertheless, these small changes are capable of leading to a wide variation in $\bar{R}_h$ values (32–60 Å). Similarly, the addition of a third hydroxyl group to the steroid nucleus causes $\Delta\mu°$ for the TC micelle (in 0.6 M NaCl) to be 3 kcal/mol less negative than that for the TDC or TCDC bile salts and thus appreciably

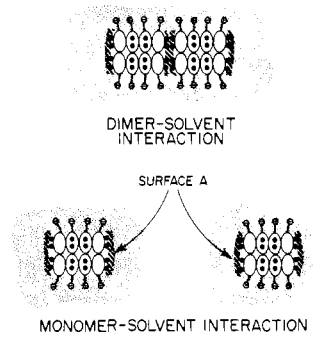

FIGURE 12: Schematic diagram of micelle–solvent interactions. Upper figure represents solvent interacting with a secondary micelle "dimer". Lower figures represent solvent interacting with two primary micelles (denoted as "monomers"). Note that when primary micelles dimerize the solvent loses contact with the two cross-hatched surfaces denoted by A.

reduces the tendency for the TC primary micelles to form secondary micelles. If one considers now the negative enthalpy changes, the value for TDC is the largest in magnitude followed by TCDC, TUDC, and TC and is not markedly dependent on the NaCl concentration (as expected from the slopes of the ln K vs. T^{-1} plots). With regard to the $\Delta S°$ values, these vary in their sign from species to species, but in all cases they show an increase as the NaCl concentration is raised. Finally, it is seen that the effect of added urea in the TDC system is to produce less negative $\Delta\mu°$ values by virtue of a reduction in the magnitude of $\Delta H°$, which is partially compensated by an increase in $\Delta S°$.

Roles of Electrostatic Repulsion, Hydrogen Bonding, and Hydrophobic Interactions in the Formation of Secondary Micelles. In this section we offer a quantitative interpretation of the above thermodynamic data in terms of a simple conceptual picture of the micelle–micelle and micelle–solvent interactions that are involved in the formation of secondary micelles. We begin by writing a theoretical expression for $\Delta\mu°$ in which the contributions of electrostatic repulsion, hydrogen bonding, and micelle–solvent interactions are explicitly identified (eq 18), where (1) $\Delta\mu_{El}$ represents the free energy

$$\Delta\mu° = \Delta\mu_{El} + \Delta\mu_{H\ bond} + \Delta\mu_{solvation} + \Delta\mu_{HI} \quad (18)$$

of electrostatic repulsion (a positive quantity) that must be overcome when two charged primary micelles and their surrounding ionic atmospheres are brought into contact, (2) $\Delta\mu_{H\ bond}$ is the free-energy change (a negative quantity) associated with intermicellar hydrogen bonding between the hydroxyl groups on the micellar surfaces, (3) $\Delta\mu_{solvation}$ is the free-energy difference associated with the solvation of primary and secondary micelles, and (4) $\Delta\mu_{HI}$ represents the free energy of hydrophobic interactions associated with the dimerization of primary micelles. The physical meaning of the last two terms is readily appreciated by considering the schematic diagram of micelle–solvent interactions shown in Figure 12. From this figure it is seen that the dimerization of primary micelles results in a loss of micelle–solvent contact in those regions of the micellar surface (denoted A) which become opposed when the primary micelles bind. As a result the solvation of the hydrophilic hydroxyl groups on the A surface (presumably a hydrogen-bond interaction between H_2O and the OH groups) will be lost during dimerization and $\Delta\mu_{solvation}$ will therefore be a positive quantity. Conversely, it should also be appreciated that although the A surfaces represent the hydrophilic sides of the bile salt molecules, inspection of Stuart–Briegleb molecular models reveals that there still is a considerable amount of *hydrocarbon* exposed to solvent

contact on this surface. The elimination of this hydrocarbon–water interface upon dimerization will therefore be accompanied by a favorable (negative value) free-energy change, $\Delta\mu_{HI}$, associated with hydrophobic interactions.

From eq 18 it thus follows that the formation of secondary micelles is favored by two factors, intermicellar hydrogen bonding, $\Delta\mu_{H\ bond}$, and hydrophobic interactions, $\Delta\mu_{HI}$, whereas the dissociation of the secondary micelle is favored by the electrostatic repulsive energy, $\Delta\mu_{El}$, and the solvation term, $\Delta\mu_{solvation}$. Small (1968) has previously suggested that intermicellar hydrogen bonding may be the major force promoting secondary micelle formation; however, we believe this is unlikely for two reasons. First, there is strong evidence to suggest that in aqueous systems the tendency of solutes to associate by hydrogen bonding is greatly diminished by the formation of equally strong solute–solvent hydrogen bonds (Klotz & Franzen, 1962; Schrier et al., 1964). In terms of eq 18 this implies that the solvent–hydroxyl interaction included in the term $\Delta\mu_{solvation}$ should be comparable in magnitude to the intermicellar hydrogen bonding, $\Delta\mu_{H\ bond}$. As a result, the sum $\Delta\mu_{H\ bond} + \Delta\mu_{solvation}$ should be close to zero and thus contributes little to the net stability of the secondary micelle. Secondly, if hydrogen bonding were the principle driving force for secondary micelle formation, it would be difficult to understand why TC micelles which contain three hydroxyl groups per bile salt polymerize to a lesser degree than the dihydroxy bile salt micelles. From these considerations it would seem that the principle driving force for secondary micelle formation must be the repulsive hydrophobic interaction between the solvent and the surface of the primary micelle. The following order of magnitude calculation shows that the observed values of $\Delta\mu°$ in 0.6 M NaCl are quantitatively consistent with this idea. If one takes the sum $\Delta\mu_{H\ bond} + \Delta\mu_{solvation}$ to be zero and neglects the term $\Delta\mu_{El}$ (which will be justified later), it follows from eq 18 that $\Delta\mu°$ will be approximately equal to $\Delta\mu_{HI}$. According to Reynolds et al. (1974) the magnitude of $\Delta\mu_{HI}$ should be given by eq 19, where

$$\Delta\mu_{HI} = -2\gamma_{HI}A \qquad (19)$$

γ_{HI} is an empirically deduced proportionality coefficient between the hydrophobic repulsive free energy and the area of hydrocarbon–water interface and A is the area of hydrocarbon on each primary micelle which is presumed to be removed from water contact when dimerization occurs. Taking the value of $\Delta\mu_{HI}$ to be 20 (cal/mol)/Å^2 (Reynolds et al., 1974), we find that our most negative value of $\Delta\mu$, −6.7 kcal/mol (obtained for TDC), could be accounted for with a value of A equal to ~168 Å^2. This value would seem quite reasonable as it is comparable to the area of hydrocarbon–water contact on the hydrophilic surface of the bile salt monomer (estimated from a Stuart–Briegleb molecular model)[6] and suggests that the binding of primary micelles involves contact between one bile salt molecule on each micelle. On this basis we conclude that the growth of bile salt micelles is a further attempt on the part of the system to produce structures which minimize the unfavorable contact between hydrocarbon and water, analogous to the growth of typical detergent micelles (Tanford, 1972; Mazer et al., 1976).

The discussion above serves as a basis for quantitatively understanding the influences of bile salt species, NaCl concentration, and urea concentration on the $\Delta\mu°$ values. In the case of bile salt species, we postulate that the number and location of hydroxyl groups on the steroid nucleus of each bile salt influence the effective area of hydrocarbon–water contact on the hydrophilic surface, thereby affecting the value of A and hence the magnitude of $\Delta\mu_{HI}$. Applying a similar analysis as was done for TDC micelles, we find that the $\Delta\mu°$ values (20 °C, 0.6 M NaCl) for the other bile salt species imply A values equal to (TC) 95, (TUDC) 138, and (TCDC) 160 Å^2 as compared to the 168 Å^2 obtained for TDC. From these values it is appreciated that the TC micelles polymerize less than the dihydroxy bile salts because their extra hydroxyl group reduces the A value by 30–40% as compared to the dihydroxy species. It is of interest that the particular ordering of the dihydroxy bile salt species with respect to micellar size exactly parallels their relative chromatographic mobilites as measured by reverse-phase liquid chromatography (Bloch & Watkins, 1978). In this way our deductions of the hydrocarbon–water interfacial area A for the three dihydroxy species correlate well with their hydrophilic–hydrophobic partioning, as inferred by chromatography, and provide additional support for the role of hydrophobic interactions in the formation of secondary micelles.

Table II: Calculations of the Free Energy of Electrostatic Repulsion

NaCl (M)	l_D (Å)[a]	$\Delta\mu_{El}$ (kcal/mol at 20 °C)
0.15	7.77	1.98
0.6	3.89	0.36
0.6 (+6 M urea)	4.31	0.38
3.0	1.74	0.03

[a] Debye length.

The effect of NaCl concentration on the $\Delta\mu°$ values is expected to occur principally through the electrostatic repulsion term $\Delta\mu_{El}$. Using the Verwey–Overbeek theory (1968) of the electrical interaction between spherical double layers, we have derived the expression shown in eq 20 for $\Delta\mu_{El}$ (see Appendix B), where (1) Z is the charge on the primary micelle, (2) r_o

$$\Delta\mu_{El} = \left[\frac{Z^2}{16\pi r_o^3 C_{NaCl}} \ln\left(1 + e^{-S/l_D}\right)\right] RT \qquad (20)$$

is the radius of the primary micelle, (3) C_{NaCl} is the added NaCl concentration (molecules/cm^3), (4) S is the distance of separation between the micellar surfaces in the secondary micelle, (5) RT is the thermal energy, and (6) l_D is the double-layer thickness (or Debye length) which is dependent on NaCl concentration (see Appendix B). Using values for Z of 10 and r_o of 15 Å, consistent with our deductions of the size and aggregation number of primary micelles, and choosing a reasonable value for S of 3 Å, we have used eq 20 to estimate $\Delta\mu_{El}$ as a function of NaCl concentration, as seen in Table II. These data show that as the NaCl concentration increases from 0.15 to 0.6 M, $\Delta\mu_{El}$ decreases from 1.98 to 0.36 kcal/mol, a value which is indeed small compared to the overall magnitude of $\Delta\mu°$. This 1.62 kcal/mol reduction in $\Delta\mu_{El}$ parallels the experimental dependence of $\Delta\mu°$ on NaCl concentration, in which a decrease of 1.6–2.1 kcal/mol was observed for the dihydroxy bile salts as the NaCl concentration was increased from 0.15 to 0.6 M (Table I). This finding supports our contention that the main effect of NaCl (at these concentrations) is to decrease the electrostatic repulsion between the primary micelles. However, at the very high NaCl concentration employed in the study of TC micelles (3.0 M), NaCl must also be influencing the micelle–solvent interactions as

[6] This area does not correspond to the interfacial (projection) area of the bile salt monomer as measured from surface tension studies (Kratohvil & DelliColli, 1968) but instead represents an estimate of the total *cavity surface area* between hydrocarbon and water on the hydroxylated side of the steroid nucleus.

Table III: Comparison of $\Delta\mu^\circ - \Delta\mu^n$ with Free Energy of Transfer Data

molarity of urea	0	0.5	2	4	6
$\Delta\mu^\circ - \Delta\mu^n$ (cal/mol)[a]		−300	−1000	−1600	−1800
Δf_t for phenylalanine (cal/mol)[b]		−50	−180	−330	−470
Δf_t for tryptophan (cal/mol)[b]		−75	−270	−500	−730
γ_{HI} ((cal/mol)/Å^2)	20	19.1	17.0	15.2	14.6

[a] From data of Table I. [b] From Nozaki & Tanford (1963).

well, in that the predicted reduction in $\Delta\mu_{El}$ to 0.03 kcal/mol (Table II) is not enough to explain the observed decrease in $\Delta\mu^\circ$ (Table I).

While there are a number of possible mechanisms (not necessarily exclusive of each other) by which urea could be influencing the $\Delta\mu^\circ$ values, we shall discuss here only one such mechanism based on the effect of urea on hydrophobic interactions. From measurements of the relative solubilities of amino acids in water and aqueous urea solutions, Nozaki & Tanford (1963) have deduced the free energy of transferring certain amino acid side groups between these solvents and have concluded from their data that the repulsive free energy of hydrophobic interactions is diminished by the addition of urea to the aqueous solutions. On this basis we would expect the value of $\Delta\mu_{HI}$ to decrease in magnitude with added urea and thus reduce the driving force for secondary micelle formation. If one assumes this to be the sole effect of urea (note from Table II that urea has little effect on $\Delta\mu_{El}$), it would follow from eq 18 and 19 that the difference between $\Delta\mu^\circ$ for TDC micelles in 0.6 M NaCl and $\Delta\mu^\circ$ in 0.6 M NaCl with "n" molar urea is given by eq 21a–c, where the superscript "n"

$$\Delta\mu^\circ - \Delta\mu^n = \Delta\mu_{HI} - \Delta\mu_{HI}^n \quad (21a)$$

$$= (-2A\gamma_{HI}) - (-2A\gamma_{HI}^n) \quad (21b)$$

$$= -2A(\gamma_{HI} - \gamma_{HI}^n) \quad (21c)$$

denotes the molarity of urea in the solvent. Equation 21b shows that $\Delta\mu^\circ - \Delta\mu^n$ is in essence the hypothetical free-energy cost of transferring a hydrocarbon–water interface of area $2A$ from water to "n" molar urea solution. In Table III, we therefore compare our experimental deductions of $\Delta\mu^\circ - \Delta\mu^n$ as a function of urea concentration, with the numerical values of the free energy of transfer (Δf_t) for the hydrophobic amino acid side groups, phenylalanine and tryptophan, taken from Nozaki & Tanford (1963). We see that our values of $\Delta\mu^\circ - \Delta\mu^n$ are roughly 3–5 times larger in magnitude than the Δf_t values, a result consistent with the smaller size of the amino acid side groups in relation to the hydrophilic surface of the bile salt molecule ($A \approx 168$ Å^2 for TDC). This consistency supports our hypothesis that urea decreases the tendency of primary micelles to polymerize by virtue of decreasing the hydrophobic interactions between the solvent and the micellar surface. On this basis, we have employed our deductions of $\Delta\mu^\circ - \Delta\mu^n$ in conjunction with eq 21c to deduce the dependence of γ_{HI} on urea concentration, as shown in Table III. In this way we have quantified the influence of urea on hydrophobic interactions and have found that in 6 M urea solution γ_{HI} has a value of 14.65, a 27% reduction from its value in water.

Enthalpy of Secondary Micelle Formation. To conclude our thermodynamic analysis of bile salt aggregation we shall briefly consider the significance of the enthalpy changes deduced in Table I. In analogy with eq 18, we can decompose the experimental ΔH° value into the contributions that electrostatic repulsion, hydrogen bonding, solvation, and hydrophobic interactions make to it (eq 22). The first term,

$$\Delta H^\circ = \Delta H_{El} + \Delta H_{H\ bond} + \Delta H_{solvation} + \Delta H_{HI} \quad (22)$$

ΔH_{El}, can be estimated using the theoretical expression for $\Delta\mu_{El}$ given in eq 20. As $\Delta\mu_{El}$ is essentially proportional to T in this expression (the weak temperature dependence of l_D is negligible), it follows from eq 17a that ΔH_{El} will be zero and can therefore be discarded from eq 22. This result is consistent with our experimental finding that the ΔH° values are roughly independent of NaCl concentration. Moreover, from our earlier discussion about hydrogen bonding in aqueous solution it is also expected that $\Delta H_{H\ bond} + \Delta H_{solvation} \approx 0$. Having eliminated the first three terms of eq 22, we are forced to identify ΔH° with the term ΔH_{HI}. As the experimental ΔH° values vary from −2 to −9 kcal/mol and comprise the major negative contribution to the $\Delta\mu^\circ$ values, this would imply that the hydrophobic driving force for secondary micelle formation, $\Delta\mu_{HI}$, is largely enthalpic in origin; that is, heat is given off as the hydrocarbon–water interface on the primary micelle is reduced by dimerization. This finding differs from the view first proposed by Frank & Evans (1945) and further developed by others (Tanford, 1972) that hydrophobic interactions arise largely from unfavorable entropic effects associated with the ordering of water molecules around a hydrocarbon solute, with only a small or positive enthalpy effect (favoring the interaction of water and hydrocarbon). Although it is beyond the scope of this paper to fully reconcile this difference, we do wish to point out that these disparate views emerge from considerations of quite different systems. On the one hand, our deductions of $\Delta\mu_{HI}$ relate to the process of polymerization of primary bile salt micelles and reflect the exclusion of water from hydrocarbon contact on the adjoining surfaces. On the other hand, the data of Frank & Evans relate to the relative solubilities of small hydrocarbon and rare gas molecules in water vs. organic solvents. Such measurements reflect the different chemical potentials of these small molecules in the two solvents.

Our deductions as to the enthalpic contributions to hydrophobic effects in micellar systems receive support from other data as well. First, we note that the enthalpy of primary micelle formation, ΔH_M, as derived from the temperature dependence of the cmc of bile salt solutions (Carey & Small, 1969) indicates that between 20 and 60 °C micelle formation is an enthalpically driven process (i.e., $\Delta H_M \approx -1$ to -5 kcal/mol). As we have attributed the cmc phenomenon to the formation of primary micelles in which the hydrophobic surfaces of the bile salt molecules lose contact with the solvent, the ΔH_M values would be consistent in sign and magnitude with our conclusion that the exposure of hydrocarbon to the solvent is enthalpically unfavorable. Additional support for the present finding is provided by recent studies of the thermodynamics of sodium dodecyl sulfate ($NaDodSO_4$) micelle formation (Mazer et al., 1977), in which the temperature-dependent growth of spherical $NaDodSO_4$ micelles into cylindrically shaped aggregates was shown to be driven by hydrophobic interactions at the micelle–water interface (i.e., between the head groups on the micelle surface) that were largely enthalpic in origin. In fact, a quantiative estimate of the enthalpy of hydrophobic interaction, as derived from the $NaDodSO_4$ data, gave a value of −20 (cal/mol)/Å^2 of hydrocarbon–water interface. If this value is multiplied by 336 Å^2 (twice the area, A, on each primary TDC micelle surface which becomes apposed during polymerization), we obtain an estimate for ΔH° of −6.7 kcal/mol, which is in good agreement with our experimental value for secondary TDC micelle formation. In this manner, we have found that the large

enthalpy effects which drive micellar growth in both the bile salt and $NaDodSO_4$ systems can each be attributed to an unfavorable hydrophobic interaction at the micelle–water interface of magnitude 20 (cal/mol)/Å^2. The generality of this effect and its relation to other experimental data on hydrophobic interactions clearly warrant further investigation.

Acknowledgments

We thank Jean Wu and Grace Ko for their excellent technical assistance in purifying the bile salt species used in this study. We are most grateful to Dr. Hirotsune Igimi (Peter Bent Brigham Hospital) for providing a highly pure sample of TCDC and to Dr. John Watkins (Children's Hospital Medical Center) for allowing us to use his reversed-phase, high-performance liquid chromatograph. We also acknowledge many helpful discussions with Drs. Donald Small, Charles Young, Richard Cohen, and Sum P. Lee. Finally, a special thanks goes to Teri Fox, who typed the manuscript.

Appendix A

Calculations of $\bar{R}_h$ and V as a Function of KC_o/n_o. Equations 1–4 were employed to calculate $\bar{R}_h$ and V as a function of KC_o/n_o. Such calculations require specifying the fraction of the scattered light intensity, G_i, the diffusion coefficient, D_i, and the scattering form factor, P_i, corresponding to the primary micelle ($i = 1$) and each secondary micelle species ($i = 2, 3, \ldots$). The dependence of G_i on KC_o/n_o is obtained from eq 2 through the dependence of the micellar concentrations C_i (weight/volume) on KC_o/n_o as given by eq 12 and 15. Combining these results, we obtain eq A-1. D_i

$$G_i = \frac{(in_o)^2[1 - [(4KC_o/n_o + 1)^{1/2} - 1]/(2KC_o/n_o)]^i P_i}{\sum_{i=1} (in_o)^2[1 - [(4KC_o/n_o + 1)^{1/2} - 1]/(2KC_o/n_o)]^i P_i} \quad \text{(A-1)}$$

values were calculated from the hydrodynamic radii R_i of each micellar species using the Stokes–Einstein relation (eq A-2).

$$D_i = kT/6\pi\eta R_i \quad \text{(A-2)}$$

For the purposes of calculating R_i and P_i, each micellar species was modeled as an ellipsoid with a semiminor axis of 15 Å and an axial ratio equal to i (the number of primary micelles contained in the secondary micelle). This is consistent with the rodlike structure deduced for the secondary micelles. The relevant equations for R_i and P_i are found in Tanford (1961). A Nova 1200 computer was used to calculate the sums given in eq 1, A-1, and 4. Convergence of the sums was assured by utilizing a sufficient number of terms such that a running sum of $n_oX_{n_o} + \sum_{i=2}(n_oi)X_{n_oi}$ had reached 99% of C_o.

Appendix B

Calculations of the Free Energy of Electrostatic Repulsion, $\Delta\mu_{El}$. As $\Delta\mu_{El}$ theoretically represents the free-energy cost of bringing two charged primary micelles from infinite separation to a small distance between the micellar surfaces, it may be equated with the Verwey–Overbeek potential energy function $V(S)$ (where S is the distance of separation between the micellar surfaces in the secondary micelle). This function, in the limit where the double-layer thickness (or Debye length), l_D, is small compared to the radius of the primary micelle, r_o, is given by eq B-1 (Verwey & Overbeek, 1968), where $\epsilon(T)$

$$V(S) = \frac{\epsilon(T)r_o\psi_o^2}{2} \ln(1 + e^{-S/l_D}) \quad \text{(B-1)}$$

is the dielectric constant of the solvent and ψ_o is the electric potential on the surface of the micelle. In this same limit ($l_D << r_o$), ψ_o will be approximately equal to that shown by eq B-2, where Ze is the charge on the micelle. The Debye length

$$\psi_o \approx \frac{Ze}{\epsilon(T)r_o}\left(\frac{l_D}{r_o}\right) \quad \text{(B-2)}$$

itself is defined by eq B-3,

$$l_D = \left(\frac{\epsilon(T)kT}{8\pi C_{NaCl}e^2}\right)^{1/2} \quad \text{(B-3)}$$

where C_{NaCl} is the concentration of added NaCl ions (i.e., NaCl) in ions/cm^3 and kT is the thermal energy. Combining eq B-1, B-2, and B-3, one obtains the result identified as $\Delta\mu_{El}$ in eq 20.

References

Admirand, W. H., & Small, D. M. (1968) *J. Clin. Invest. 47*, 1043.
Bloch, C. A., & Watkins, J. B. (1978) *J. Lipid Res. 19*, 510.
Borgström, B. (1965) *Biochim. Biophys. Acta 106*, 171.
Carey, M. C. (1975) *N. Engl. J. Med. 293*, 1255.
Carey, M. C., & Small, D. M. (1969) *J. Colloid Interface Sci. 31*, 382.
Carey, M. C., & Small, D. M. (1970) *Am. J. Med. 49*, 590.
Carey, M. C., & Small, D. M. (1972) *Arch. Intern. Med. 130*, 506.
Carey, M. C., & Small, D. M. (1978) *J. Clin. Invest. 61*, 998.
Chu, B. (1974) *Laser Ligh Scattering*, Academic Press, New York.
Cohen, R. J., & Benedek, G. B. (1976) *J. Mol. Biol. 108*, 151.
Cummins, H. Z., & Pike, E. R. (1974) *Photon Correlation and Light Beating Spectroscopy*, Plenum Press, New York.
Cummins, H. Z., & Pike, E. R. (1977) *Photon Correlation Spectroscopy and Velocimetry*, Plenum Press, New York.
Debye, P. (1949) *Ann. N.Y. Acad. Sci. 51*, 575.
DelliColli, H. T. (1970) Ph.D. Thesis, Clarkson College, New York.
Dietschy, J. M. (1968) *J. Lipid Res. 9*, 297.
Djavanbakht, A., Kale, K. M., & Zana, R. (1977) *J. Colloid Interface Sci. 59*, 139.
Ekwall, P., Fontell, K., & Sten, A. (1959) *Proc. Int. Congr. Surf. Act., 2nd, 1957 1*, 357.
Fontell, K. (1971) *Kolloid Z. Z. Polym. 246*, 614.
Frank, H. S., & Evans, M. W. (1945) *J. Chem. Phys. 13*, 507.
Holzbach, R. T., Oh, S. Y., McDonnell, M. E., & Jamieson, A. M. (1977) in *Micellization, Solubilization and Microemulsions* (Mittal, K. L., Ed.) Vol. 1, p 403, Plenum Press, New York.
Klotz, I. M., & Franzen, J. S. (1962) *J. Am. Chem. Soc. 84*, 3461.
Koppel, D. E. (1972) *J. Chem. Phys. 57*, 4814.
Kratohvil, J., & DelliColli, H. T. (1968) *Can. J. Biochem. 46*, 945.
Laurent, T. C., & Persson, H (1965) *Biochim. Biophys. Acta 106*, 616.
Makino, I., Shinozaki, K., Yoshino, K., et al. (1975) *Nippon Shokakibyo Gakkai Zasshi 72*, 690.
Matschiner, J. T. (1976) in *The Bile Acids* (Nair, P. P., & Kritchevsky, D., Eds.) Vol. 1, p 11, Plenum Press, New York.
Mazer, N. A. (1973) S.B. Thesis, Massachusetts Institute of Technology, Cambridge, MA.
Mazer, N. A. (1978) Ph.D. Thesis, Massachusetts Institute of Technology, Cambridge, MA.

Mazer, N. A., Benedek, G. B., & Carey, M. C. (1976) *J. Phys. Chem. 80*, 1075.
Mazer, N. A., Carey, M. C., & Benedek, G. B. (1977) in *Micellization, Solubilization and Microemulsions* (Mittal, K. L., Ed.) Vol. 1, pp 359–381, Plenum Press, New York.
McCrea, L. F., & Angerer, S. (1960) *Biochim. Biophys. Acta 42*, 344.
Mittal, K. L., Ed. (1977) *Micellization, Solubilization and Microemulsions*, Vol. 1, pp 383–403, Plenum Press, New York.
Moore, W. J. (1962) *Physical Chemistry*, 3rd ed., Prentice-Hall, Englewood Cliffs, NJ.
Mukerjee, P. (1972) *J. Phys. Chem. 76*, 565.
Mukerjee, P., & Cardinal, J. R. (1976) *J. Pharm. Sci. 65* 882.
Nozaki, Y., & Tanford, C. (1963) *J. Biol. Chem. 238*, 4074.
Olson, J. A., & Herron, J. S. (1966) *Proc. Int. Congr. Biochem., 6th, 1964 7*, 588.
Ramonathan, N., Currie, A. L., & Colvin, J. R. (1961) *Nature (London) 190*, 779.
Reynolds, J. A., Gilbert, D. B., & Tanford, C. (1974) *Proc. Natl. Acad. Sci. U.S.A. 71*, 2925.
Rich, A., & Blow, D. M. (1958) *Nature (London) 182*, 423.
Sabotka, H., & Czeczowezka, N. (1958) *J. Colloid Sci. 13*, 188.
Schrier, E. E., Pottle, M., & Scheraga, H. A. (1964) *J. Am. Chem. Soc. 86*, 3444.
Sehlin, R. C., Cussler, E. L., & Evans, D. F. (1975) *Biochim. Biophys. Acta 388*, 385.
Small, D. M. (1967) *Gastroenterology 52*, 607.
Small, D. M. (1968) *Adv. Chem. Ser. No. 84*, 31.
Small, D. M., Bourgês, M., & Dervichian, D. G. (1966) *Nature (London) 211*, 816.
Tanford, C. (1961) *Physical Chemistry of Macromolecules*, Wiley, New York.
Tanford, C. (1969) *Adv. Protein Chem. 23*, 121.
Tanford, C. (1972) *The Hydrophobic Effect*, Wiley, New York.
Verwey, E. J. W., & Overbeek, J. Th. G. (1968) *Theory of the Stability of Lyophobic Colloids*, Elsevier, Amsterdam.
Vitello, L. (1971) Ph.D. Thesis, Clarkson College, New York.
Woodford, F. P. (1969) *J. Lipid Res. 10*, 539.

Synthesis and Spectral Properties of a Hydrophobic Fluorescent Probe: 6-Propionyl-2-(dimethylamino)naphthalene†

Gregorio Weber* and Fay J. Farris

ABSTRACT: Environmentally sensitive fluorescent probes involve two groups, an electron donor and an electron acceptor, attached to an aromatic ring system, and maximal effects may be expected when these groups are as far apart as feasible. The synthesis, characterization, and spectroscopic properties of 6-propionyl-2-(dimethylamino)naphthalene (PRODAN), a compound that fulfills these conditions, are described. The maximum of emission is at 401 nm in cyclohexane solution and at 531 nm in water solution, indicating an increase of dipole moment of ~20 D units on excitation to the lowest singlet state. The effect of temperature upon the spectral distribution and the bandwidth of fluorescence of PRODAN in 1:1 complexes with albumin shows the existence of a dynamic relaxation process of the protein surroundings within the 2–4 ns of the fluorescence lifetime.

The red shift of the fluorescence spectrum with increasing polarity of the solvent environment has been the object of both theory and experiment (Oochika, 1954; Lippert, 1957; Bakhshiev, 1964). It is agreed that this red shift is dependent upon a large increase in dipole moment in the fluorescent state over that of the ground state, and it is possible to foresee qualitatively the possibility of such enhancement of the dipole moment on excitation for some aromatic structures. The fluorescence from the unsubstituted aromatic hydrocarbons may be expected to show little sensitivity to the environment on account of the high degree of symmetry of the ground and lowest singlet excited states (e.g., Platt, 1964). The attachment to the aromatic ring system of two groups which are respectively a good electron donor and a good electron acceptor results in a lowest excited state with an important charge-transfer character that results from loss of charge by the donor group and its gain by the acceptor. The most important potential donor is the amino or alkylamino group, and the best acceptors are probably the S=O and C=O groups. The attachment of these groups at different points of the aromatic ring structure produces similar, though not identical, results, and at present a wholly empirical approach to these secondary effects seems the most advisable course in planning the synthesis of suitable polarity-sensitive fluorescent molecules. However, other things being equal, we can expect strongest effects when the distance between donor and acceptor groups is a maximum. In a naphthalene derivative this condition is fulfilled when donor and acceptor groups are attached to the 2 and 6 positions of the rings.

This paper describes a general method for the preparation of 2-(dimethylamino)-6-acylnaphthalenes, substances which offer outstanding sensitivity of the fluorescence to the polarity of the environment, and reports some of the properties of one member of the family, 6-propionyl-2-(dimethylamino)-naphthalene (PRODAN).[1]

† From the Biochemistry Department, University of Illinois, Urbana, Illinois 61801. *Received February 6, 1979.* This work was supported by Grant 11223 of the National Institute of General Medical Sciences, U.S. Public Health Service.

[1] Abbreviations used: PRODAN, 6-propionyl-2-(dimethylamino)-naphthalene; PROMEN, 6-propionyl-2-methoxynaphthalene; ANS, 8-anilino-1-naphthalenesulfonic acid; bis(ANS), 4,4′-bis(1-anilino-8-naphthalenesulfonic acid); HMPA, hexamethylphosphoramide.

0006-2960/79/0418-3075$01.00/0